Excited-state lifetime studies of the three tryptophan residues in the N-lobe of human serum transferrin

Nicholas G. James,[1]* Justin A. Ross,[2] Anne B. Mason,[1] and David M. Jameson[2]

[1]Department of Biochemistry, University of Vermont, College of Medicine, Burlington, Vermont 05405
[2]Department of Cell and Molecular Biology, John A. Burns School of Medicine, University of Hawaii, Honolulu, Hawaii 96813

Received 14 August 2009; Revised 21 September 2009; Accepted 26 October 2009
DOI: 10.1002/pro.287
Published online 20 November 2009 proteinscience.org

Abstract: The energy transfer from the three Trp residues at positions 8, 128, and 264 within the human serum transferrin (hTF) N-lobe to the ligand to metal charge transfer band has been investigated by monitoring changes in Trp fluorescence emission and lifetimes. The fluorescence emission from hTF N-lobe is dominated by Trp264, as revealed by an 82% decrease in the quantum yield when this Trp residue is absent. Fluorescence lifetimes were determined by multifrequency phase fluorometry of mutants containing one or two Trp residues. Decays of these samples are best described by two or three discrete lifetimes or by a unimodal Lorentzian distribution. The discrete lifetimes and the center of the lifetime distribution for samples containing Trp128 and Trp264 are affected by iron. The distribution width narrows on iron removal and is consistent with a decrease in dynamic mobility of the dominant fluorophore, Trp264. Both the quantum yield and the lifetimes are lower when iron is present, however, not proportionally. The greater effect of iron on quantum yields is indicative of nonexcited state quenching, *i.e.*, static quenching. The results of these experiments provide quantitative data strongly suggesting that Förster resonance energy transfer is not the sole source of Trp quenching in the N-lobe of hTF.

Keywords: time-resolved fluorescence; lifetime distribution; tryptophan fluorescence; FRET; human serum transferrin

Introduction

Fluorescence spectroscopy is an extremely sensitive technique that has provided a wealth of insight into biological processes. Fluorescence can be monitored using either extrinsic (covalent or noncovalent) or intrinsic (tryptophan, tyrosine, phenylalanine, flavin adenine dinucleotide, reduced nicotinamide adenine dinucleotide, *etc*) fluorophores.[1–5] Spectroscopic characterization of a fluorophore's excitation/emission spectra, quantum

Additional Supporting Information may be found in the online version of this article.

Abbreviations: FRET, Förster resonance energy transfer; hTF, human serum transferrin; hTF N-lobe, recombinant N-lobe of human serum transferrin comprising residues 1-337; LMCT, ligand to metal charge transfer; WT, wild-type; W8, the double mutant in the hTF N-lobe containing the W128Y/W264Y mutations; W8Y, the hTF N-lobe wherein Trp8 has been replaced by a Tyr residue; W128, the double mutant in the hTF N-lobe containing the W8Y/W264Y mutations; W128Y, the hTF N-lobe wherein Trp128 has been replaced by a Tyr residue; W264, the double mutant in the hTF N-lobe containing the W8Y/W128Y mutations; W264Y, the hTF N-lobe wherein Trp264 has been replaced by a Tyr residue.

Nicholas G. James' current address is Department of Cell and Molecular Biology, John A. Burns School of Medicine, University of Hawaii, 651 Ilalo Street, Biosciences 222, Honolulu, Hawaii 96813.

Grant sponsor: USPHS; Grant number: R01 DK21739; Grant sponsor: Hemostasis and Thrombosis Training; Grant number: 5T32HL007594.

*Correspondence to: Nicholas G. James, Department of Cell and Molecular Biology, John A. Burns School of Medicine, University of Hawaii, 651 Ilalo Street, Biosciences 222, Honolulu, Hawaii 96813. E-mail: njames4@hawaii.edu

yield, polarization/anisotropy, and lifetime(s), provides critical information regarding the photophysics of the system and the interactions of the fluorophore with its environment.[6,7] The exceptional sensitivity of some fluorophores to changes in local environment has been exploited to monitor biological processes such as ligand binding, protein unfolding, and protein-protein interaction.[8–12] Although Förster resonance energy transfer (FRET) is the only fluorescence technique that provides direct structural information, conformational changes in biological molecules can be inferred from alterations in a fluorophore's emission properties. The nature of these changes can only be determined if the molecular origins of the changes in fluorescence are identified.

Trp residues are the least common amino acid in proteins and typically dominate the fluorescence of a given protein.[13,14] Hence, they are the most commonly used intrinsic fluorophores. The fluorescence emission from Trp residues is extremely sensitive to changes in local environment (~30-fold variation in quantum yield and ~50 nm change in emission maxima).[15] As indicated earlier, this sensitivity has been exploited to monitor numerous biological processes; however, the inability to pinpoint the causes of changes in the fluorescence yield limits the informational content of such measurements.[8,9,15,16] Further complications in interpretation of the changes in fluorescence at a molecular level are added if there is more than one Trp in a protein. In some cases, this complication can be circumvented by using site-directed mutagenesis to generate single-Trp containing mutants allowing assignment of spectral changes in the wild-type (WT) protein to an individual Trp residue.[9] However, the well-known stabilizing effect of Trp residues on protein structure sometimes precludes such a strategy.[17] For example, mutation of one of the five Trp residues in the C-lobe of human serum transferrin (hTF), Trp358, apparently results in destabilization, leading to very little protein expression.[18]

Another confounding problem associated with Trp fluorescence is that often the lifetime decay of even single-Trp containing proteins exhibits complex patterns.[9] Determination of the lifetime(s) of Trp residues yields information about excited state interactions. Several models have been proposed to describe the lifetime heterogeneity observed for individual Trp residues within proteins. The "classical rotamer model" contends that different ground state conformers of Trp, which exist on a longer timescale than the lifetime of the excited state, have different interactions within the protein matrix, thus producing distinct lifetimes.[19,20] More recently, Rolinski *et al*.[21] have presented a Langevin-equation based refinement of the rotamer model to account for observed nonexponentiality of Trp lifetimes. The "solvent/spectral relaxation model" suggests that the heterogeneity is due to the increase in the dipole moment of the excited state that produces short-lived "blue" and long-lived "red" species that combine to produce the steady-state emission.[22] Although knowledge of the lifetimes can provide valuable information on the environment surrounding Trp residues, interpretation of results from these studies has been hindered by the complexity of the decay data.

Changes in the intrinsic fluorescence emission of hTF have been used to provide insight into the mechanism of iron binding/release and the association of hTF with the specific transferrin receptor.[23,24] Physiologic transport of iron (and possibly other metals) in humans occurs primarily through binding of hTF to its receptor and endocytosis of the complex.[25] Like all members of this family, hTF is a single-chain polypeptide (679 amino acids) that folds to form two homologous iron-binding lobes termed the N- and C-lobe.[26] These lobes are further subdivided into two subdomains, NI/NII and CI/CII, which are connected by a hinge forming a central cavity suitable for iron binding. In each lobe, four protein ligands (Asp63, Tyr95, Tyr188, and His249 hTF N-lobe numbering) and two oxygen ligands from the synergistic anion carbonate provide high affinity iron coordination in a distorted octahedral geometry.[27]

The isolated hTF N-lobe (residues 1–337) can be recombinantly expressed in large quantities and has been shown to be structurally equivalent to the N-lobe of full-length hTF.[28,29] Iron binding to the hTF N-lobe causes a ~3-fold reduction in the intrinsic fluorescence emission.[30] The quenching of the intrinsic fluorescence has been modeled as excited state energy transfer (or FRET) from the Trp residues to an absorption band created by iron binding.[31] This ligand to metal charge transfer (LMCT) band, which is observed in the visible region (centered at 470 nm) and in the UV (250–400 nm), results when the π-orbitals of the liganding Tyr residues merge with the *d*-orbital of the iron atom creating a new orbital delocalized between the Tyr and iron.[32] To investigate how each residue is affected by iron coordination, the three Trp residues, located at positions 8, 128, and 264 (Fig. 1), were mutated to create a full array of double and single-Trp containing mutants.[30,34] In our previous work, kinetic analysis of iron release (carried out by monitoring the increase in Trp fluorescence) at pH 5.6 (in the presence of the chelator ethylenediaminetetraacetic acid (EDTA) and absence of salt) from the hTF N-lobe and the Trp mutants, yielded biphasic kinetics that was modeled as (1) iron release and (2) conformational relaxation.[34] If FRET is the only source of quenching, a single fluorescent event should be observed. The biphasic kinetics of iron release indicate that one or more of the three the Trp residues undergo changes in quantum yield associated with

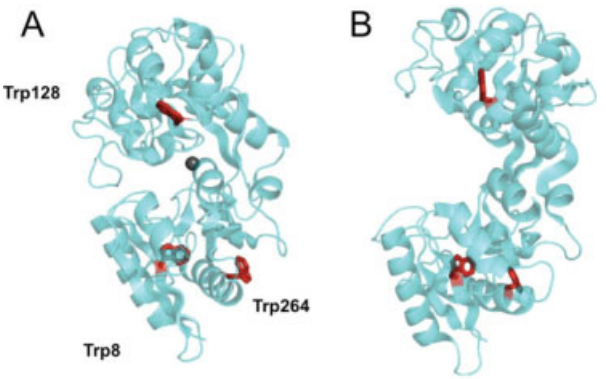

Figure 1. Crystal structures of hTF N-lobe in both the iron bound (A [PDB ID: 1A8E]) and apo (B [PDB ID: 1BP5]) states showing the location of each of the three Trp residues (highlighted in red) and the large conformational change in the N-lobe associated with iron removal. This figure was made using PyMol.[33] [Color figure can be viewed in the online issue, which is available at www.interscience.wiley.com.]

structural alterations during cleft opening (*i.e.*, enhanced interaction with nearby residues).

Since its first description in 1969, the prevailing dogma for the mechanism of Trp quenching in iron-bound hTF is FRET between the Trp residues and the LMCT absorbance band.[31,35,36] Even though the quenching of intrinsic fluorescence has been proposed to be FRET (an excited-state process), no direct information about the excited state for the individual Trp residues of the hTF N-lobe is available. In this work, steady-state emission spectra, quantum yields and polarizations of WT hTF N-lobe, single point Trp mutants (W8Y, W128Y, and W264Y), and double Trp mutants in which only the Trp indicated remains (W8, W128, and W264) were determined with and without iron bound. Excited-state lifetimes were obtained for the WT protein and each of the six mutants in the apo and iron-bound state using multifrequency phase and modulation fluorometry. The efficiency of energy transfer to the LMCT band was calculated for each Trp residue based on spectral data from each mutant (assuming that the changes in spectral properties were solely due to FRET). Excited-state lifetimes for Trp128 and Trp264 indicate substantial differences in their local environments between apo and iron-bound states, clearly demonstrating non-FRET mediated changes in the quantum yield of these residues. Because the quantum yield and lifetime changes upon iron release are not proportional, we propose that ground state interactions, such as static quenching by iron coordination, account for a portion of the fluorescence quenching.

Results

Excitation polarization

The ratio of polarization when samples are excited at 295–305 nm (selective excitation of Trp) and 270–275 nm (excitation of Tyr and Trp) provides an approximation of energy transfer among aromatic amino acids. This polarization ratio has been found to be 1.4–1.5 in proteins that do not undergo Tyr-Trp energy transfer.[12] When energy transfer takes place between these residues (which decreases the polarization observed from the Trp due to non-alignment of the donor and acceptor dipoles), this ratio increases to 1.7–2.0.[12,37,38] The 300/275 polarization ratio was determined for each hTF N-lobe construct to determine whether energy transfer from Tyr to Trp residues occurs in this protein. The ratios of apo and iron-bound WT hTF N-lobe is 1.37 and 1.42, respectively. The ratios for the single (W8Y, W128Y, and W264Y) and double (W8, W128, and W264) mutants ranges between 1.36 and 1.55 in the apo form and 1.17–1.70 in iron-bound protein. The iron-bound single mutant W264Y has a ratio of 1.70 strongly indicating that Tyr-Trp energy transfer is likely taking place in this mutant. Therefore, we selected 300 nm as the excitation wavelength to avoid this transfer and any possible contamination of Tyr in the emission scans and during lifetime decay analysis.

Steady-state Trp fluorescence/quantum yields

Fluorescence emission spectra for apo and iron-bound WT hTF N-lobe, and the single (W8Y, W128Y, and W264Y) and double (W8, W128, and W264) Trp mutants are shown in Supp Figure 1. The emission intensities that are plotted were normalized to the calculated quantum yield (Φ) values (Table I). A center of mass calculation (Table I) was also used because the spectra for the iron containing samples were very broad, making it difficult to specify λ_{max} with certainty. Reporting both the center of mass as well as the change in λ_{max} also provides more information because changes in the bandwidth and/or spectral shape are taken into account.[39]

Comparison of the Trp fluorescence spectral parameters (λ_{max} and center of mass) for each Trp mutant to the WT N-lobe reveals that the W8Y, W128Y single mutants, and the W128 double mutant all have similar emission spectra (in both iron-bound and iron-free states), whereas the W264Y single mutant, W8, and the W264 double mutants show large differences in one or both states (Fig. 2 and Table I). Interestingly, in contrast to the other samples, the W8 mutant (missing both Trp128 and Trp264) spectrum does not reach the baseline beyond 380 nm (see Discussion section). Analysis of the iron-bound and apo emission spectra demonstrates that iron removal produces a 3-nm blue shift (184 cm^{-1}) in the WT hTF N-lobe. Those mutants containing Trp128 undergo the largest shifts in λ_{max} and center of mass. Specifically, the W264Y mutant undergoes a 14-nm blue shift and 803 cm^{-1} change in the center of mass. Consistent with previously reported

Table I. *Fluorescence Parameters for hTF N-Lobe, Single, and Double Trp Mutants Excited at 300 nm*

hTF N-lobe	λ_{max} (nm)	Center of mass (cm^{-1})	Φ[a]	% Difference (steady-state)[b]
WT (apo)	333	28881	0.025 ± 0.001	292
WT (Fe)	336	28694	0.006 ± 0.001	
W8Y (apo)	333	28734	0.029 ± 0.002	327
W8Y (Fe)	334	28369	0.007 ± 0.001	
W128Y (apo)	335	28566	0.017 ± 0.001	131
W128Y (Fe)	333	28506	0.007 ± 0.001	
W264Y (apo)	330	28102	0.005 ± 0.001	223
W264Y (Fe)	344	27299	0.002 ± 0.001	
W8 (apo)	336	27615	0.003 ± 0.001	−20
W8 (Fe)	340	27585	0.004 ± 0.001	
W128 (apo)	332	28258	0.020 ± 0.001	102
W128 (Fe)	338	28065	0.010 ± 0.001	
W264 (apo)	337	28599	0.025 ± 0.001	156
W264 (Fe)	338	28554	0.010 ± 0.001	

[a] Average of at least three different experiments.
[b] Calculated from $100 \times [\Phi_{Apo} - \Phi_{iron}]/\Phi_{iron}$.

observations,[30,34] mutants with Trp8 (W8) and Trp264 (W128Y and W264) show relatively small changes in emission spectra associated with iron release.

In transitioning from iron bound to apo, the Φ value of WT N-lobe increases by 292%, and the three single mutants W8Y, W128Y, and W264Y increase by 327%, 131%, and 223%, respectively, whereas the W8 double mutant decreases by 20% and the double mutants W128 and W264 increase by 102% and 156%. These values deviate slightly from previously reported changes obtained using 280 and 295 nm excitation.[30,34] Summation of the Φ values of the three double mutants, containing only Trp8, Trp128, and Trp264, does not equal that of the apo WT hTF N-lobe. Introduction of multiple Trp mutations likely cause local perturbations around the remaining Trp residues, slightly altering their interaction with their respective microenvironments (Table I). It is clear that the single Trp mutants W8Y, W128Y and

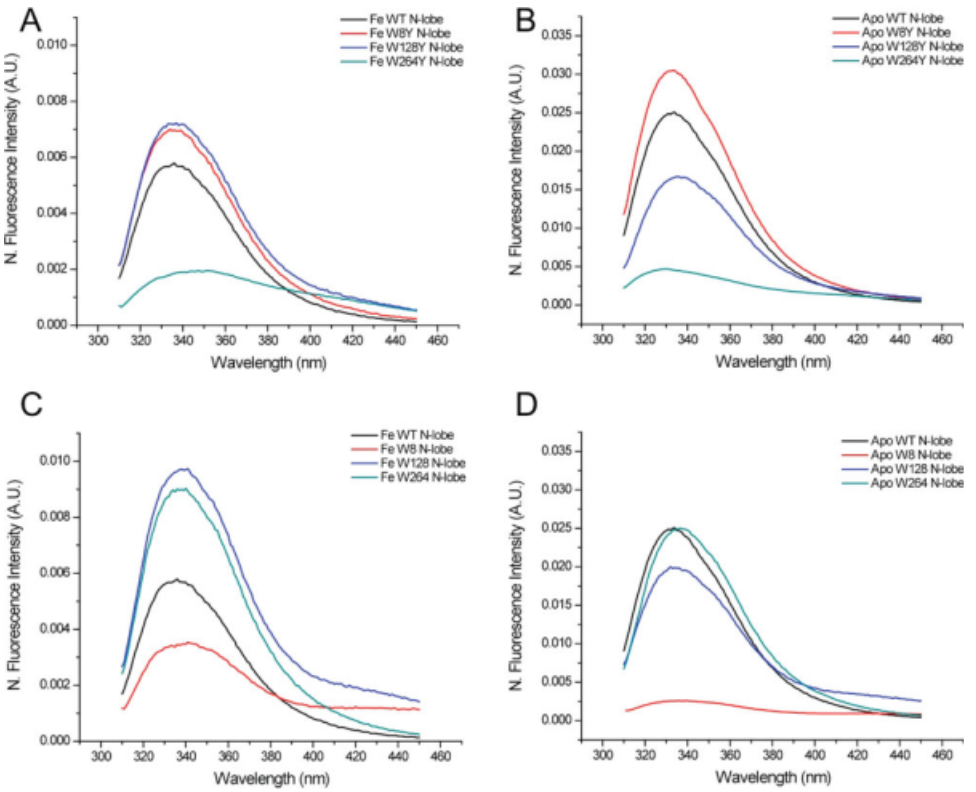

Figure 2. Steady-state emission spectra of iron bound (A) and apo (B) WT and the three single point Trp mutants. Overlay of the WT N-lobe and the three double mutants in iron bound (C) and apo (D) states. Emission scans were generated using 300 nm as the excitation wavelength and monitoring between 310 and 450 nm.

W264Y most accurately represent the Trp in their native environment.

Fluorescence lifetimes

Phase and modulation lifetimes for each N-lobe mutant in the apo and iron-bound conformation were determined at 15 different frequencies ranging from 35 to 300 MHz. The apo conformation of the WT hTF N-lobe shows a shift of the phase and modulation data to lower frequencies [SupFig1. (A)], demonstrating an increase in excited state lifetime, similar to what is observed for the steady-state data. As described in the Materials and Methods section, the data were analyzed using Globals software (Laboratory of Fluorescence Dynamics, UC Irvine) to fit to a single, double, and triple exponential decay (with a small scattering component) to obtain f_i (fractional contribution to the total intensity), α_i (pre-exponentials), and τ_i [Table II and SupFig. 1(B–G)]. Although data from some of the constructs fit well to a double exponential decay, the iron-bound single mutant W264Y and the double mutants W8 and W128 (iron-bound) fit better to a triple exponential function.

Fitting to an exponential model assumes that the Trp residues are emitting from a single protein conformation(s).[9] Alternatively, as detailed in the introduction,[40,41] Trp lifetimes can be analyzed as continuous distributions rather than as discrete emitting species, potentially providing information on local conformation and dynamics.[12,42,43] Thus, as shown in Table III, each mutant can be modeled by a single Lorentzian distribution with one discrete component with reduced chi-squared values similar to the double and triple exponential models. The center of the distribution for iron bound WT is 1.45 ns with a width of 1.34 ns. The absence of iron leads to a shift in the distribution, with the center at 3.34 ns and the width decreasing to 0.83 ns [Table III and Fig. 3(A)]. Significantly, the lifetime distribution of any mutant containing Trp264 undergoes large decreases in the width associated with iron removal.

Fe-FRET efficiency

The quenching of Trp residues by iron bound to hTF has been proposed to be due to FRET between the Trp residues and the iron-Tyr LMCT band.[31] The Förster distance (R_0) for each Trp residue was calculated based on the overlap of their fluorescence emission (in the absence of iron) and their LMCT when iron is bound. The distance between each Trp residue and the iron center was determined from the iron-bound crystal structure (Table IV). Calculated efficiencies based on steady-state data [Eq. (4)], lifetime data [Eq. (5)], and structural data [Eq. (6)] are presented in Table IV, with the assumption that any change in spectral data is due to energy transfer. Based on its location, Trp8 is predicted to undergo little energy transfer ($E_{Calc} = 0.11$) when iron is present, and the spectral data confirm that no quenching of this residue takes place in the presence of iron. Any change in the spectral properties of the double mutant W8 is likely to result from photodegradation products, such as disulfide reduction (see Discussion section). Trp128, located in the iron binding cleft (Fig. 1), is predicted to be the most affected by iron binding and therefore, to undergo the most energy transfer to the iron binding center ($E_{Calc} = 0.77$). However, the experimental efficiencies (0.51 and 0.38) were considerably lower than the calculated efficiency. Although Trp264 is furthest away from the iron binding center (21 Å) (Fig. 1), we have clearly shown that its fluorescence emission is quenched when iron is bound.[34] The efficiency of energy transfer of this residue to the LMCT band is predicted to be 0.20; however, experimental efficiencies of 0.61 and 0.36 are obtained using steady-state and lifetime data.

With the assumption that Trp8 is weakly fluorescent and not contributing to the change in the emission on iron binding, we analyzed the FRET efficiency of the single mutants W128Y and W264Y assuming that they more accurately represent Trp264 and Trp128, respectively. The results of this analysis are presented in Table IV. The predicted energy transfer from Trp128 (W264Y) is almost half of what is predicted from the double mutant containing only Trp128 (0.43 *vs*. 0.77). Efficiencies of 0.68 and 0.51 were found for this mutant under steady-state and lifetime conditions. The theoretically calculated efficiency for Trp264 in the W128Y mutant, ($E_{Calc} = 0.12$), was significantly lower than the observed values (0.57 and 0.24 for steady-state and lifetime data, respectively). Similar to their double mutant counterparts, W128Y and W264Y had higher efficiencies of energy transfer when the steady-state data was compared to the time-resolved results.

Discussion

Interpretation of quantum yields of hTF N-lobe mutants

The total Φ value of all three Trp residues in the isolated iron free hTF N-lobe is 0.025 ± 0.001. This extremely low Φ suggests that all of the Trp are efficiently quenched even in the absence of metal binding. Trp8 is located in a hydrophobic box surrounded by two disulfide bonds (Cys9/Cys48 and Cys19/Cys39) and has been shown to interact with two water molecules [Fig. 4(A)]. Continuous excitation of the mutant containing only Trp8 (W8) at 295 nm leads to an enhancement in the fluorescence emission, which led to the hypothesis that Trp8 interacts with and stabilizes these disulfide bonds.[34] Disulfide bonds have been shown to quench Trp fluorescence via excited state electron transfer.[16] The Trp8

Table II. *Discrete Lifetime Analysis of Each Mutant With and Without Iron*[a]

hTF N-lobe	τ_1 (ns)	τ_2 (ns)	τ_3 (ns)	α_1	α_2	α_3	τ_{ave} Ampl. (ns)	χ^2
WT (apo)	3.92	1.61	—	0.60	0.40	—	2.99	2.73
WT (Fe)	4.44	1.23	—	0.10	0.90	—	1.55	1.20
W8Y (apo)	4.13	1.66	—	0.59	0.41	—	3.12	3.21
W8Y (Fe)	4.95	1.33	—	0.13	0.87	—	1.80	2.17
W128Y (apo)	4.02	1.37	—	0.67	0.33	—	3.15	3.15
W128Y (Fe)	5.95	1.44	—	0.21	0.79	—	2.39	2.24
W264Y (apo)	4.75	1.58	—	0.20	0.80	—	2.21	2.60
W264Y (Fe)	7.81	2.58	0.36	0.03	0.23	0.74	1.09	1.27
W8 (apo)	7.69	3.28	0.84	0.04	0.29	0.66	1.82	3.10
W8 (Fe)	5.51	2.26	0.53	0.15	0.30	0.55	1.80	1.24
W128 (apo)	4.78	1.37	—	0.32	0.68	—	2.46	2.88
W128 (Fe)	5.64	1.94	0.26	0.15	0.27	0.58	1.52	0.96
W264 (apo)	4.34	1.32	—	0.61	0.39	—	3.16	2.29
W264 (Fe)	5.01	1.29	—	0.20	0.80	—	2.03	1.25

[a] A fixed value for the standard errors of the phase and modulation (0.3° and 0.006 for phase angle and demodulation ratio, respectively) were used when analyzing the data.

construct has an extremely low Φ value (~0.003) and shows minimal change in emission when removed by mutation (the W8Y mutant). Consistent with our previous conclusions, this residue contributes minimally to the overall fluorescence emission.[30,34]

Trp128 resides deep within the iron binding cleft and is nearest to the iron binding center (Fig. 1). We predict that the fluorescence from the W264Y single mutant is originating almost entirely from Trp128. If this is the case, then Trp128 in this context shows a 4-fold enhancement (apo protein) in its fluorescence signal upon mutation of Trp8 (the difference between the W264Y single mutant and the W128 double mutant). Although energy transfer between Trp residues can decrease fluorescence emission, Trp8 and Trp128 would not be predicted to undergo energy transfer because the critical transfer distance for Trp homotransfer is approximately 6 to 12 Å[44] but they are separated by ~20–30 Å in the apo and iron bound state, respectively.[38] A more likely explanation is that mutation of Trp8 produces alterations in the structure, resulting from its interactions with the disulfide bonds, and causes subtle changes in the microenvironment of Trp128. This destabilizing effect has been previously observed as indicated by a difference in the rate constant from iron release of each mutant.[34] We suggest that the actual Φ value of Trp128 in WT hTF N-lobe is more accurately reflected by the W264Y construct (0.005).

Examination of the residues surrounding Trp128 provides some insight into its low Φ value. Two residues, His119 and Asn129, have been identified as possible quenchers of Trp128 [Fig 4(B)]. His119 lies ~6 Å away from Trp128 (in both states) and mutational studies (H119A and H119Q) have proven that this residue contributes to the low Φ of Trp128.[30] Quenching of Trp fluorescence by protonated histidines has been documented by a mechanism involving ground state interaction.[16] The δO of Asn129 lies parallel to the indole side chain of Trp128 and ~4 Å away from the NH group and

Table III. *Analysis of Lifetime Data With a Lorentzian Distribution and One Discrete (D) Component*[a]

hTF N-lobe	F_1	Center (ns)	Width (ns)	F_2	D (ns)	χ^2
WT (apo)	0.98	3.34	0.83	0.02	0.53	2.55
WT (Fe)	0.99	1.45	1.34	0.01	0.001	1.19
W8Y (apo)	0.93	3.59	0.89	0.07	1.67	2.15
W8Y (Fe)	0.99	1.78	1.91	0.01	0.001	1.97
W128Y (apo)	0.93	3.85	0.28	0.08	0.79	1.88
W128Y (Fe)	0.72	4.47	1.72	0.28	0.96	2.81
W264Y (apo)	0.98	2.43	1.76	0.02	0.58	1.72
W264Y (Fe)	0.68	3.23	1.36	0.32	0.25	2.73
W8 (apo)	0.84	3.18	2.12	0.16	0.49	2.32
W8 (Fe)	0.84	3.36	2.22	0.16	0.33	1.54
W128 (apo)	0.91	3.28	2.17	0.09	0.71	1.95
W128 (Fe)	0.91	3.59	2.28	0.09	0.31	2.00
W264 (apo)	0.92	4.10	0.36	0.08	0.82	2.12
W264 (Fe)	0.69	3.60	1.93	0.31	1.03	3.30

[a] A fixed value for the standard errors of the phase and modulation (0.3° and 0.006 for phase angle and demodulation ratio, respectively) were used when analyzing the data.

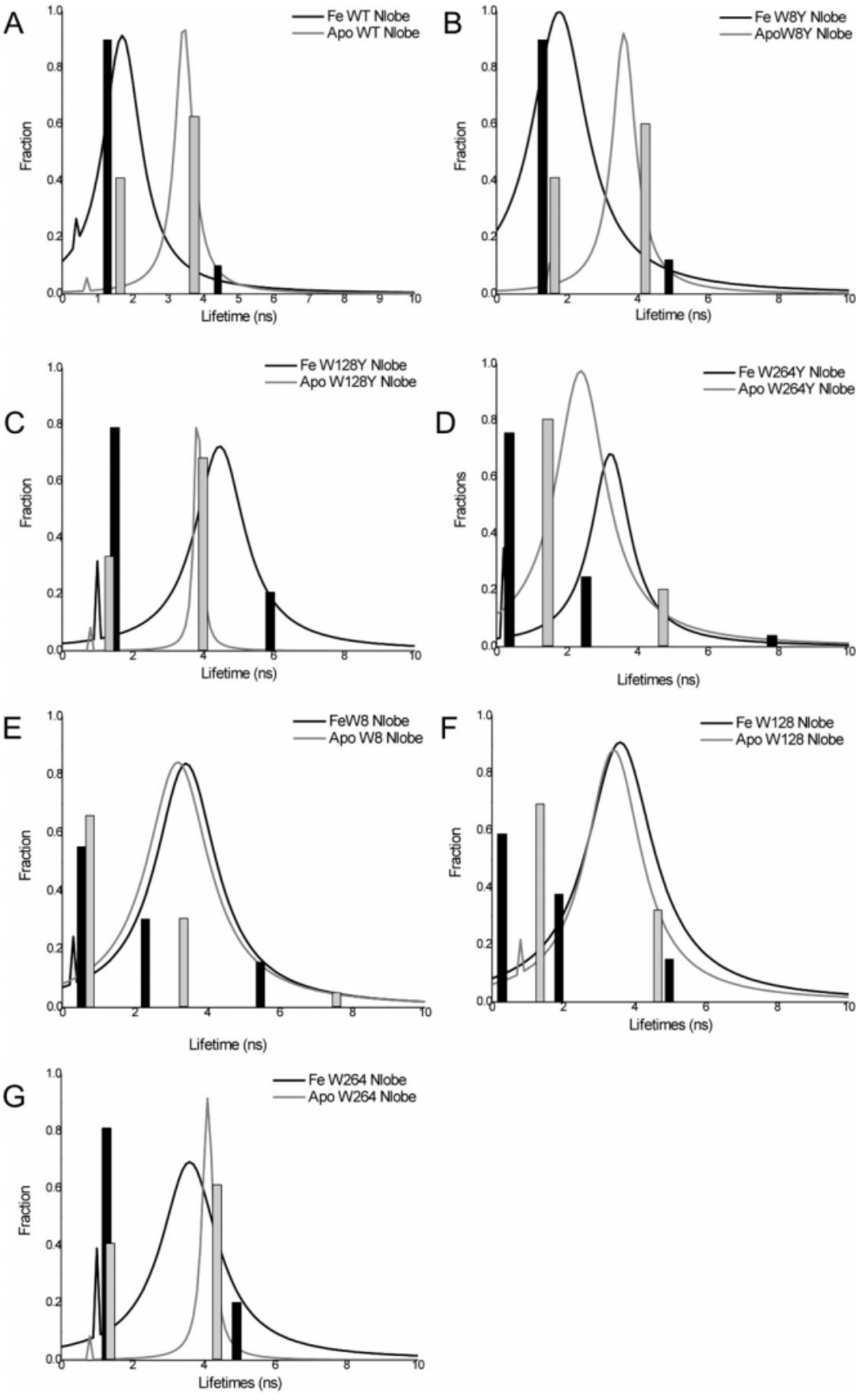

Figure 3. Lorentzian distribution of apo and iron bound lifetimes overlaid with the discrete components: (A) WT N-lobe, (B) W8Y, (C) W128Y, (D) W264Y, (E) W8, (F) W128, and (G) W264. Each Lorentzian distribution was calculated with one discrete component.

Table IV. *Förster Resonance Energy Transfer Parameters of Trp (donor) and Iron-Tyr (acceptor)*

Trp residue	Φ_D	$J(\lambda)$ ($\times 10^{-15}$ cm^3·M^{-1})	R_0 (Å)[a]	R (Å)	$E_{(SS)}$[b]	$E_{(LT)}$[c]	$E_{(Calc)}$[d]
W8	0.003	5.42	11.4	16	−0.27	0.01	0.11
W128	0.020	5.03	16.0	13	0.51	0.38	0.77
W264	0.025	4.24	16.2	21	0.61	0.36	0.20
W264Y	0.005	5.23	12.4	13	0.68	0.51	0.43
W128Y	0.017	4.69	15.1	21	0.57	0.24	0.12

[a] κ^2 assumed to be 2/3.
[b] Calculated from steady-state data using Eq. (4).
[c] Calculated from discrete lifetime data (Table 2) using Eq. (5).
[d] Calculated from Eq. (6). Distances between Trp residues (^1L_A transitions) and the iron center were determined from the iron-bound crystal structure of hTF N-lobe (PDB 1A8E).

could either quench Trp128 via electron transfer or stabilize the charge transfer state with its amide backbone. Changes in solvent accessibility around Trp128 could also contribute to its fluorescence emission. A water molecule is in close proximity to the indole in the apo state and interacts with the εNH group of the indole on iron binding [Fig. 4(B)]. Trp interactions with water have been shown to have profound affects on fluorescence emission.[45,46] Any (or all) of these factors undoubtedly influence and stabilize the charge transfer state of Trp128 reducing the effective quantum yield.[15,46,47]

Located on the surface on α-helix-9 of the NI subdomain, Trp264 contributes the most to the emission spectra (5-fold decrease in Φ in W264Y) (Table I). Like Trp128, the difference between the Φ of W128Y (emission solely from Trp264) and the double mutant W264 is probably due to structural alterations that occur when Trp8 is mutated. The quenching mechanism for this residue is difficult to assign, because the indole ring is sandwiched between two residues, Lys304 and Asn268 [Fig. 4(C)]. The ζNH of Lys304 lies 4.5 Å away from the pyrrole ring and could quench the fluorescence by excited-state proton transfer.[16] The Asn268 lies close to the indole ring of Trp264 with several water molecules surrounding it and could serve to quench the fluorescence of Trp264 through electron transfer.

Lifetime analysis

Iron binding clearly reduces the intrinsic protein fluorescence intensity of the N-lobe of hTF. This

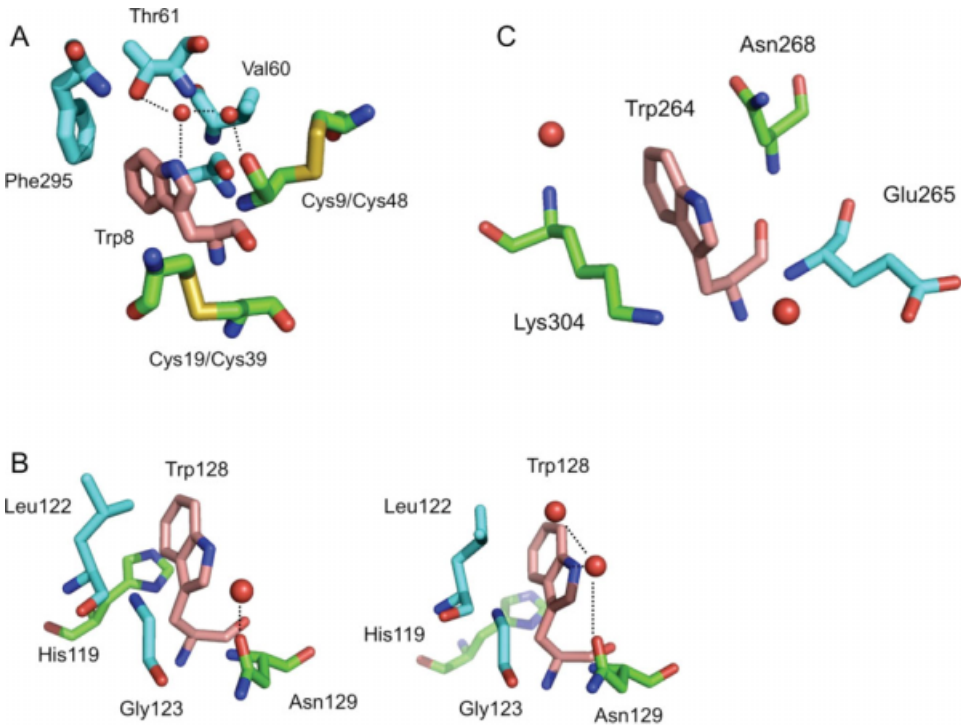

Figure 4. Positions of hTF N-lobe Trp from apo (PDB ID: 1BP5) and iron bound (1A8E) structures. (A) Close-up view of Trp8 surrounded by two disulfide bonds (Cys9/Cys48 and Cys19/Cys39), Val60, Thr61, and Phe295 and two water molecules (red spheres). (B) Close-up view of the change in local environment of Trp128 in the iron bound and apo states. (C) Close-up view of the local environment of Trp264. This figure was made using PyMol.[33] [Color figure can be viewed in the online issue, which is available at www.interscience.wiley.com.]

reduction in intensity is also accompanied by a reduction in the average fluorescence lifetime (Tables II and III, Sup Fig. 1 and Fig. 3). Even in the case of the mutants retaining a single Trp residue, the lifetime data does not fit well to a single, discrete exponential decay. This result is not surprising, because most single Trp containing proteins exhibit complex lifetime decays.[48] As shown in Figure 3 and Table III, the results for the single Trp constructs of both apo and iron-bound hTF N-lobe fit reasonably well to Lorentzian distributions, which reflects not only the intrinsic excited state lifetime of the Trp residue but also the dynamics of that residue as it samples different protein environments in both the ground and excited state.[41] Interestingly, the distribution profile for the apo *versus* iron containing W128Y and W264 becomes very narrow [Fig. 3(C,G)], indicating that the dynamics of this residue are significantly altered. As described by Alcala *et al.,*[43] more complex distributions, including skewed-Lorentzian models, may be a more appropriate way to consider Trp residues within a protein. However, caution is warranted in interpreting lifetimes, *per se*, regardless of the analysis. In transitioning from apo to iron-bound the overall structures of these proteins are markedly different, with the subdomains undergoing a $\sim 63^{\circ}$ movement. Thus the precise environment of each Trp residue is likely to differ, resulting in different excited state lifetime parameters and altered Φ values.

FRET analysis

The single point mutants W128Y and W264Y and the double mutants W128 and W264 all have higher efficiencies of energy transfer from the steady-state data compared to the time-resolved data. Although quenching by a FRET process by the iron is certainly possible, as shown by calculations of the R_0's and average distances of donor and acceptor (Table IV), it is probably not reasonable to assume that a simple FRET model can account for the excited state properties of the iron-bound form of the protein. Therefore, we conclude that conformational changes associated with cleft closure cause these residues to form ground state complexes with the protein matrix and/or iron binding may function as a static quencher. Both of the proposed events would cause a decrease in the steady-state emission of the Trp residues without causing a change in the excited-state lifetimes. The lifetime distribution profiles show a broad distribution of Trp conformations in the iron-bound state which likely produce alternate quenching/FRET patterns among the different conformers. Such a distribution would mean that some states are more efficient in energy transfer and/or alternative quenching, whereas other conformers would produce less efficient quenching from FRET or other processes.

Materials and Methods

Materials

Dulbecco's modified Eagle's medium-Ham F-12 nutrient mixture, antibiotic-antimycotic solution (100×), and trypsin were from the GIBCO-BRL Life Technologies Division of Invitrogen. Fetal bovine serum was obtained from Atlanta Biologicals. Ultroser G is a serum replacement from Pall BioSepra (Cergy, France). The QuikChange mutagenesis kit and pBluescriptII were from Stratagene. Methotrexate from Bedford laboratories was used for selection of plasmid containing cells. All tissue culture dishes and flasks, and Corning expanded surface roller bottles, were obtained from Fisher Scientific. Ultracel 30 kDa MWCO microcentrifuge devices were from Amicon. Ni-NTA resin came from Qiagen. Hi-prep 26/60 Sephacryl S-200HR was obtained from Amersham Pharmacia. EDTA was from the Mann Research Laboratories Inc. NTA and ferrous ammonium sulfate were from Sigma.

Mutagenesis, protein expression, and purification of hTF N-lobe and tryptophan mutants

All Trp-Tyr mutations were introduced into the pNUT vector coding for the hTF N-lobe (residues 1–337) using the QuikChange site-directed mutagenesis kit.[30,34] The mutagenic primers used to create the single (W8Y, W128Y, and W264Y) and double Trp mutations (W8, W128, and W264) in the hTF N-lobe have been previously described.[30,34,49] Incorporation of the mutagenic plasmid, protein expression, and purification followed our standard protocol.[34,50]

Steady-state fluorescence emission and quantum yield determination

Steady-state emission spectra were obtained for each hTF N-lobe construct using a Quantamaster Spectrofluorimeter (Photon Technology International, South Brunswick NJ).[34] Quantum yields (Φ) of each sample were determined using a L-tryptophan standard ($\Phi = 0.14$).[51] Samples were excited at 300 nm, and emission scans were monitored from 310 to 450 nm, using slit widths of 5 nm (excitation) and 5 nm (emission). The excitation wavelength was polarized parallel to the laboratory axis, and emission wavelength was observed through two polarizer settings: (1) parallel and (2) perpendicular. Total fluorescence intensity was obtained using the equation:

$$I_T = I_{II} + 2I_{\perp} \quad (1)$$

where $I_{\parallel}$ and $I_{\perp}$ are the fluorescence intensities observed through parallel and perpendicular polarizers, respectively.[11] All spectra were corrected for Raman scattering and background fluorescence by subtraction of the appropriate buffer blank. Iron

containing protein (3 μ*M*, A_{300} ~0.05) was added to a cuvette (1.8 mL final volume) containing 100 m*M* HEPES buffer, pH 7.4, at 20°C and gently stirred with a small magnetic stir bar. The concentration for each construct, apo and iron bound, was determined using the molar absorption coefficients previously reported.[34,52] Apo protein was generated by adding the identical amount of iron protein to 100 m*M* MES, pH 5.6 containing 4m*M* EDT, and equilibrating for ~20 minutes (room temperature) before addition to a cuvette, stirring at 20°C. Three steady-state emission scans were collected and averaged. Individual Φ_{prot} were calculated using the following equation[51]:

$$\Phi_{prot} = \Phi_{Trp} \times \left(\frac{I_{prot}}{I_{Trp}}\right) \times \left(\frac{1 - 10^{-A(Trp)}}{1 - 10^{-A(prot)}}\right) \quad (2)$$

Φ_{Trp} is the quantum yield of the L-tryptophan standard (0.14), I_{prot} and I_{Trp} are the integrated fluorescence intensities [area under the curve for I_T from Eq. (1)] of mutant and L-tryptophan standard and A_{prot} and A_{Trp} are the absorbance of the mutant and L-tryptophan standard at the excitation wavelength 300 nm.

Polarization studies

Steady-state fluorescence measurements were conducted on an ISS PC1 (ISS Inc., Champaign, IL) steady-state fluorimeter using a Xenon lamp as the excitation source with excitation and emission slit widths of 8 nm and long pass 330 nm emission filters. Apo and iron bound protein (~10 μ*M*) was maintained at 20°C. Emission spectra were recorded with the emission polarizer vertically oriented and were corrected for instrument response parameters. Total emission intensity [Eq. (1)] was measured by exciting with vertically polarized light at 275 nm or 300 nm and recording both the parallel and perpendicular emission intensities sequentially.

Multifrequency phase and modulation fluorometry experiments

Frequency domain experiments were conducted on an ISS Chronos Fluorometer using IFR 2023 frequency synthesizers and a 300-nm LED as the excitation light source (reviewed in Ref. 53). P-terphenyl (Sigma) dissolved in spectroscopic grade ethanol (Sigma) was used as the lifetime reference. Modulation frequencies were chosen such that the phase delay stayed within the range of 15°–75°. Two 330-nm long pass filters were used as emission filters for each lifetime measurement. Data were analyzed to multiexponential functions to obtain discrete lifetimes and a Lorentzian distribution model using Globals software (E. Gratton, Laboratory of Fluorescence Dyanmics). Preexponential values were obtained from the fractional fluorescence intensity (*f*) using the equation:

$$f_i = \frac{\alpha_i \times \tau_i}{\sum \alpha_i \times \tau_i} \quad (3)$$

where α_i is the preexponential (amplitude) of the decay associated with the lifetime component τ_i. All fluorescence measurements were made using ~10 μ*M* protein concentration in 10 × 4 mm quartz cuvettes (Starna Cells Inc., CA) at 20°C.

Förster resonance energy transfer between Trp-LMCT

The efficiency of energy transfer (*E*) in hTF N-lobe was experimentally determined from the decrease in Trp fluorescence (as a result of iron binding) monitored by steady-state (E_{SS}) and time-resolved (E_{LT}) data and calculated from the equations:

$$E_{SS} = 1 - \left(\frac{F_{DA}}{F_D}\right) \quad (4)$$

$$E_{LT} = 1 - \left(\frac{\tau_{DA}}{\tau_D}\right) \quad (5)$$

where F_D, F_{AD}, τ_D, and τ_{DA} are the fluorescence emission and lifetimes from the donor (Trp) in the absence and presence of the acceptor (LMCT), respectively. The efficiency of energy transfer can also be determined based on the distance separating the donor and acceptor molecule:

$$E = \frac{R_0^6}{(R_0^6 + R^6)} \quad (6)$$

where R_0 is the distance at which 50% of the energy is transferred between donor and acceptor. This distance, typically referred to as Förster distance, is calculated using the equation:

$$R_0 = 9.78 \times 10^3 \times [\kappa^2 n^{-4} \phi_D J(\lambda)]^{(1/6)} (M^{-1}\text{cm}^3) \quad (7)$$

where *n* is the refractive index of the medium (taken as 1.4[7]), Φ_D is the quantum yield of the donor in the absence of the acceptor, and $J(\lambda)$ is the overlap integral, which is calculated from the absorption spectra of the acceptor and the fluorescence emission. To calculate $J(\lambda)$, the absorption spectra was normalized to the molar absorptivity of the acceptor and the fluorescence emission of the donor was normalized to have an integrated area of 1. The geometric orientation factor (κ^2) is assumed to be 2/3 due to the isotropic symmetry of the transition of the acceptor to the donor.

Conclusion

The long-standing idea that FRET completely accounts for Trp fluorescence quenching by iron has been critically evaluated by steady-state and time-resolved measurements. The three Trp residues of

hTF (8, 128, and 264) were mutated to create constructs containing either two Trp residues or a single Trp residue(s). Although the mutants containing only one Trp residue would seem to provide the best information regarding the photophysics of individual Trp in the hTF N-lobe, spectral data suggest that mutation of Trp8 produces slight alterations in the local environment of the remaining two Trp residues. Therefore, the single Trp mutants W128Y and W264Y (each containing two remaining Trp residues) seem to provide the most accurate depiction of emission from Trp264 and Trp128, respectively. We suggest that a number of interactions with neighboring residues and the solvent matrix of each Trp residue are responsible for the low Φ value of the WT hTF N-lobe. Lifetime analysis reveals dramatic differences in the microenvironment around Trp264, which will influence its Φ of apo and iron-bound forms. This study provides quantitative evidence for alternative quenching mechanisms associated with metal binding to hTF N-lobe.

Acknowledgments

We thank Dr. Karol Gryczynski, Dr. Ignacy Gryczynski, and Shashank Bahrill (University of North Texas) for their experimentation using TCSPC and for providing insight into comparison between steady-state and time-resolved data. We also thank Dr. Dmitri Toptygin (Johns Hopkins University) for providing his software for calculating distances between residues and Drs. Stephen Everse and Shaina L. Byrne for their helpful comments made during the preparation of this manuscript.

References

1. Weber G (1952) Polarization of the fluorescence of macromolecules. I. Theory and experimental method. Biochem J 51:145–155.
2. Weber G (1952) Polarization of the fluorescence of macromolecules. II. Fluorescent conjugates of ovalbumin and bovine serum albumin. Biochem J 51:155–167.
3. Slavik J (1982) Anilinonaphthalene sulfonate as a probe of membrane composition and function. Biochim Biophys Acta 694:1–25.
4. Teale FW, Weber G (1957) Ultraviolet fluorescence of the aromatic amino acids. Biochem J 65:476–482.
5. Rancy PC, Thorpe C (2008) Oxidative protein folding in vitro: a study of the cooperation between quiescin-sulfhydryl oxidase and protein disulfide isomerase. Biochemistry 47:12047–12056.
6. Valeur B (2002) Molecular fluorescence: principles and applications. Weinheim, Germany: Wiley-VCN.
7. Lakowicz J (2006) Principles of fluorescence spectroscopy. 3rd ed. New York: Springer.
8. Eftink MR (1991) Fluorescence techniques for studying protein structure. Methods Biochem Anal 35:127–205.
9. Beechem JM, Brand L (1985) Time-resolved fluorescence of proteins. Annu Rev Biochem 54:43–71.
10. Kosinski-Collins M, King J (2003) In vitro unfolding, refolding, and polymerization of human γD crystallin, a protein involved in cataract formation. Protein Sci 12: 480–490.
11. Lasagna M, Gratton E, Jameson DM, Brunet JE (1999) Apohorseradish peroxidase unfolding and refolding: intrinsic tryptophan fluorescence studies. Biophys J 76: 443–450.
12. Jameson DM, Gratton E, Eccleston JF (1987) Intrinsic fluorescence of elongation factor Tu in its complexes with GDP and elongation factor Ts. Biochemistry 26: 3894–3901.
13. Teale FW (1960) The ultraviolet fluorescence of proteins in neutral solution. Biochem J 76:381–388.
14. Vivian JT, Callis PR (2001) Mechanisms of tryptophan fluorescence shifts in proteins. Biophys J 80:2093–2109.
15. Callis PR, Liu T (2004) Quantitative prediction of fluorescence quantum yields for tryptophan in proteins. J Phys Chem B 108:4248–4259.
16. Chen Y, Barkley MD (1998) Toward understanding tryptophan fluorescence in proteins. Biochemistry 37: 9976–9982.
17. Ross JBA, Laws WR, Shea M,Intrinsic fluorescence in protein structure analysis in protein structures. In Unversky VN,Permyakov EA, Eds. (2007) Protein structures: methods in protein structure analysis. New York: Nova Science Publishers Inc., pp 55–72.
18. James NG, Byrne SL, Streere AN, Smith VC, MacGillivray RA, Mason AB (2009) Inequivalent contribution of the five tryptophan residues in the C-lobe of human serum transferrin to the fluorescence increase when iron is released. Biochemistry 48:2858–2867.
19. Szabo AG, Rayner DM (1980) Fluorescence decay of tryptophan conformers in aqueous solution. J Am Chem Soc 102:554–563.
20. Clayton AH, Sawyer WH (1999) Tryptophan rotamer distributions in amphipathic peptides at a lipid surface. Biophys J 76:3235–3242.
21. Rolinski OJ, Scobie K, Birch DJ (2009) Protein fluorescence decay: a gamma function description of thermally induced interconversion of amino acid rotamers. Phys Rev E Stat Nonlin Soft Matter Phys 79:050901.
22. Lakowicz JR (2000) On spectral relaxation in proteins. Photochem Photobiol 72:421–437.
23. Egan TJ, Zak O, Aisen P (1993) The anion requirement for iron release from transferrin is preserved in the receptor-transferrin complex. Biochemistry 32:8162–8167.
24. Giannetti AM, Halbrooks PJ, Mason AB, Vogt TM, Enns CA, Bjorkman PJ (2005) The molecular mechanism for receptor-stimulated iron release from the plasma iron transport protein transferrin. Structure 13:1613–1623.
25. Aisen P, Enns C, Wessling-Resnick M (2001) Chemistry and biology of eukaryotic iron metabolism. Int J Biochem Cell Biol 33:940–959.
26. Wally J, Halbrooks PJ, Vonrhein C, Rould MA, Everse SJ, Mason AB, Buchanan SK (2006) The crystal structure of iron-free human serum transferrin provides insight into inter-lobe communication and receptor binding. J Biol Chem 281:24934–24944.
27. Anderson BF, Baker HM, Norris GE, Rice DW, Baker EN (1989) Structure of human lactoferrin: crystallographic structure analysis and refinement at 2.8 Å resolution. J Mol Biol 209:711–734.
28. Funk WD, MacGillivray RT, Mason AB, Brown SA, Woodworth RC (1990) Expression of the amino-terminal half-molecule of human serum transferrin in cultured cells and characterization of the recombinant protein. Biochemistry 29:1654–1660.
29. MacGillivray RT, Moore SA, Chen J, Anderson BF, Baker H, Luo Y, Bewley M, Smith CA, Murphy ME,

Wang Y, Mason AB, Woodworth RC, Brayer GD, Baker EN (1998) Two high-resolution crystal structures of the recombinant N-lobe of human transferrin reveal a structural change implicated in iron release. Biochemistry 37:7919–7928.
30. He QY, Mason AB, Lyons BA, Tam BM, Nguyen V, MacGillivray RT, Woodworth RC (2001) Spectral and metal-binding properties of three single-point tryptophan mutants of the human transferrin N-lobe. Biochem J 354:423–429.
31. Lehrer SS (1969) Fluorescence and absorption studies of the binding of copper and iron to transferrin. J Biol Chem 244:3613–3617.
32. Gaber BP, Miskowski V, Spiro TG (1974) Resonance Raman scattering from iron(III)- and copper(II)-transferrin and an iron(III) model compound. A spectroscopic interpretation of the transferrin binding site. J Am Chem Soc 96:6868–6873.
33. DeLano WL. (2008). The PyMOL Molecular Graphics System. Palo Alto, CA: DeLano Scientific LLC.
34. James NG, Berger CL, Byrne SL, Smith VC, MacGillivray RT, Mason AB (2007) Intrinsic fluorescence reports a global conformational change in the N-lobe of human serum transferrin following iron release. Biochemistry 46:10603–10611.
35. Ainscough EW, Brodie AM, Plowman JE, Bloor SJ, Loehr JS, Loehr TM (1980) Studies on human lactoferrin by electron paramagnetic resonance, fluorescence, and resonance Raman spectroscopy. Biochemistry 19: 4072–4079.
36. Chen RF (1976) The effect of metal cations on intrinsic protein fluorescence. New York: Marcel Dekker Inc, pp 573–606.
37. Weber G (1960) Fluorescence-polarization spectrum and electronic-energy transfer in proteins. Biochem J 75:345–352.
38. Moens PD, Helms MK, Jameson DM (2004) Detection of tryptophan to tryptophan energy transfer in proteins. Protein J 23:79–83.
39. Weber G, From solution spectroscopy to image spectroscopy. In Kohen E, Ed. (1989) Cell structure and function by microspectrofluorometry. New York: Academic Press Inc., pp 71–85.
40. Gratton E, Alcala JR, Marriott G (1986) Rotations of tryptophan residues in proteins. Biochem Soc Trans 14: 835–838.
41. Alcala JR, Gratton E, Prendergast FG (1987) Fluorescence lifetime distributions in proteins. Biophys J 51: 597–604.
42. Alcala JR, Gratton E, Prendergast FG (1987) Resolvability of fluorescence lifetime distributions using phase fluorometry. Biophys J 51:587–596.
43. Alcala JR, Gratton E, Prendergast FG (1987) Interpretation of fluorescence decays in proteins using continuous lifetime distributions. Biophys J 51:925–936.
44. Van Der Meer BW, Coker G, ChenS-YS (1991) Resonance energy transfer: theory and data. New York: Wiley-VCH.
45. Yu H-T, Vela MA, Fronczek FR, McLaughlin ML, Barkley MD (1995) Microenvironmental effects on the solvent quenching rate in constrained tryptophan derivatives. J Am Chem Soc 117:348–357.
46. Chen Y, Liu B, Yu HT, Barkley MD (1996) The peptide bond quenches indole fluorescence. J Am Chem Soc 118:9271–9278.
47. Chen J, Flaugh SL, Callis PR, King J (2006) Mechanism of the highly efficient quenching of tryptophan fluorescence in human γD-crystallin. Biochemistry 45: 11552–11563.
48. Ross JA, Jameson DM (2008) Time-resolved methods in biophysics. 8. Frequency domain fluorometry: applications to intrinsic protein fluorescence. Photochem Photobiol Sci 7:1301–1312.
49. Luck L, Mason AB, Savage KJ, MacGillivray RA, Woodworth R (1997) ^{19}F NMR studies of the recombinant human transferrin N-Lobe and three single point mutants. Magnet Res Chem 35:477–481.
50. Mason AB, Halbrooks PJ, Larouche JR, Briggs SK, Moffett ML, Ramsey JE, Connolly SA, Smith VC, MacGillivray RT (2004) Expression, purification, and characterization of authentic monoferric and apo-human serum transferrins. Protein Expr Purif 36:318–326.
51. Chen RF (1967) Fluorescence quantum yields of tryptophan and tyrosine. Anal Lett 1:35–42.
52. James NG, Mason AB (2008) Protocol to determine accurate absorption coefficients for iron-containing transferrins. Anal Biochem 378:202–207.
53. Barbieri B, Terpetschnig E, Jameson DM (2005) Frequency-domain fluorescence spectroscopy using 280-nm and 300-nm light-emitting diodes: measurement of proteins and protein-related fluorophores. Anal Biochem 344:298–300.